Heat conduction through a trapped solid: the effect of structural changes on the thermal conductance

2007 J. Phys.: Condens. Matter 19 152201

(http://iopscience.iop.org/0953-8984/19/15/152201)

IOP FTC

IOP PUBLISHING JOURNAL OF PHYSICS: CONDENSED MATTER

J. Phys.: Condens. Matter **19** (2007) 152201 (7pp) doi:10.1088/0953-8984/19/15/152201

FAST TRACK COMMUNICATION

Heat conduction through a trapped solid: the effect of structural changes on the thermal conductance

Debasish Chaudhuri[1], **Abhishek Chaudhuri**[2] **and Surajit Sengupta**[3]

[1] Max Planck Institute for the Physics of Complex Systems, Nöthnitzer Strasse 38, 01187 Dresden, Germany
[2] Raman Research Institute, Bangalore-560080, India
[3] Satyendra Nath Bose National Centre for Basic Sciences—Block-JD, Sector-III, Salt Lake, Calcutta-700098, India

E-mail: debc@mpipks-dresden.mpg.de, abhishek@rri.res.in and surajit@bose.res.in

Received 20 December 2006, in final form 5 March 2007
Published 20 March 2007
Online at stacks.iop.org/JPhysCM/19/152201

Abstract

We study the conduction of heat across a narrow solid strip trapped by an external potential and in contact with its own liquid. Structural changes, consisting of addition and deletion of crystal layers in the trapped solid, are produced by altering the depth of the confining potential. Nonequilibrium molecular dynamics simulations and, wherever possible, simple analytical calculations are used to obtain the thermal resistance in the liquid, solid and interfacial regions (Kapitza or contact resistance). We show that these layering transitions are accompanied by sharp jumps in the contact thermal resistance. Dislocations, if present, are shown to increase the thermal resistance of the strip drastically.

(Some figures in this article are in colour only in the electronic version)

1. Introduction

The transport of heat through small and low-dimensional systems has enormous significance in the context of designing useful nanostructures [1]. Recently, it was shown [2] that a narrow solid strip trapped by an external potential [3–6] and surrounded by its own fluid relieves mechanical stress via the ejection or absorption of single solid layers [7–9] to and from the fluid. The trapping potential introduces large energy barriers for interfacial capillary fluctuations, thereby forcing the solid–liquid interfaces on either side of the solid region to remain flat. The small size of the solid also inhibits the creation of defects since the associated inhomogeneous elastic displacement fields need to relax to zero quickly at the boundaries, making the elastic energy cost for producing equilibrium defects prohibitively large. Therefore the only energetically favourable fluctuations are those that involve the transfer of *complete* layers which cause at most a homogeneous strain in the solid [2]. Such layering transitions

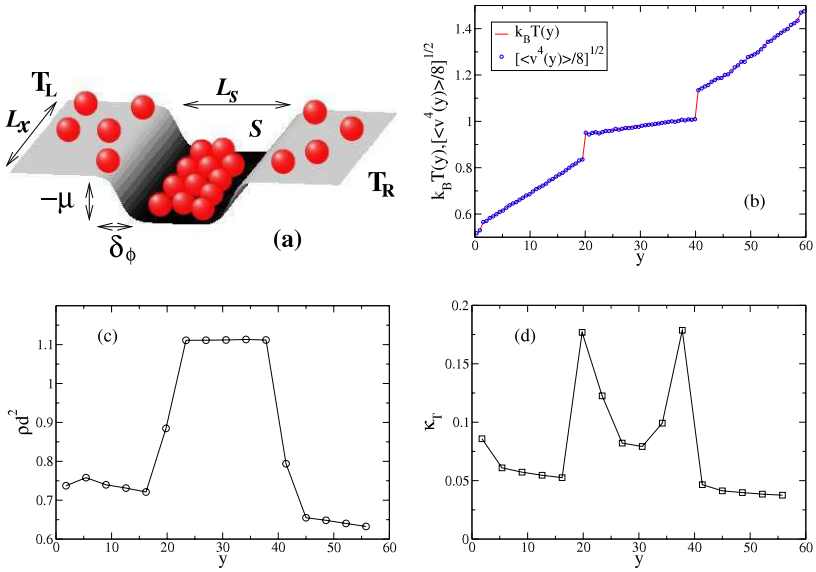

Figure 1. (a) A schematic diagram of the system showing the liquid and solid regions produced by the external chemical potential of depth $-\mu$. The various dimensions mentioned in the text are also marked in the figure. (b) Plot of the temperature profile $k_B T(y)$ and fourth moment of velocity $m\sqrt{\langle v^4(y)\rangle/8}$ at $\mu = 13$. (c) The local density profile along the y-direction at $\mu = 13$. (d) The isothermal compressibility κ_T as a function of y at $\mu = 13$. The compressibility shows strong peaks near the interfaces. Due to the small size, interfacial enhancement of the compressibility permeates right through the whole of the solid region. In (c) and (d) lines are guides to eye.

were shown to affect the sound absorption properties of the trapped solid in rather interesting ways [2]. What effect, if any, do such layering transitions have for the transfer of heat?

Heat transport across model liquid–solid interfaces has been studied in three dimensions for particles with Lennard-Jones interactions in [10] along the liquid–solid coexistence line. The dependence of the Kapitza (interfacial) resistance [11, 12] on the wetting properties of the equilibrium interface was the focus of this study. It was shown that a larger density jump at the interface causes higher interfacial thermal resistance. In this letter, we use a nonequilibrium molecular dynamics simulation to investigate heat conduction through a trapped solid (in two dimensions) as it undergoes layering transitions as a response to changes in the depth of the trapping potential. Apart from the layering transition reported in [2], we find another mode of structural readjustment, namely an increase in the number of atoms in the lattice planes parallel to the interface by the spontaneous generation and annihilation of dislocation pairs. The heat conductance, in our study, shows strong signatures of both of these structural transformations of the trapped solid.

2. System and simulation details

We consider a two-dimensional (2D) system of N atoms of average density $\rho = N/A$ within a rectangular box of area $A = L_x \times L_y$ (figure 1(a)). The applied potential, $\phi(\vec{r}) = -\mu$ for $\vec{r} \in S$ which goes to zero with a hyperbolic tangent profile of width δ_ϕ elsewhere, enhances the density ($\rho_s > \rho$) in the central region S of area $A_s = L_x \times L_s$, ultimately leading it to a solid-like phase. T_L and $T_R > T_L$ are the temperatures of the two heat reservoirs in contact with the liquid regions at either end.

A large number of recent studies in lower dimensions has shown that heat conductivity is, in fact, divergent as a function of system size [13–15]. Thus it is more sensible to directly calculate the heat current $j_E(>0)$ flowing from the high to the low temperature, or the conductance of the system $G = j_E/\Delta T$ (or resistance $R = 1/G$), $\Delta T(>0)$ being the temperature difference, rather than the heat conductivity.

We report results for 1200 particles interacting via the soft disc potential $u(r_{ij}) = 1/r_{ij}^{12}$ taken within an area of 24×60. In the absence of any external potential, a 2D system of soft discs at this density $\rho \approx 0.83$ remains in the fluid phase. The length and the energy scales are set by the soft disc diameter $d = 1$, and temperature $k_B T$, respectively, while the timescale is set by $\tau_s = \sqrt{md^2/k_B T}$. The unit of energy flux j_E is thus $(k_B T/\tau_s d)$. The units of resistance and conductance are $\tau_s d$ and $(\tau_s d)^{-1}$ respectively. Periodic boundary conditions are applied in the x-direction. We use the standard velocity Verlet scheme of molecular dynamics (MD) [16] with equal time update of time-step δt, except when the particles collide with the 'hard-walled' heat reservoirs at $y = 0$ and L_y. We treat the collision between the particles and the reservoir as that between a hard disc of unit diameter colliding against a hard, structureless wall. If the time, τ_c, of the next collision with any of the two reservoirs at either end is smaller than δt, the usual update time-step of the MD simulation, we update the system with τ_c. During collisions with the walls Maxwell boundary conditions are imposed to simulate the velocity of an atom emerging out of a reservoir at temperatures T_L (at $y = 0$) or T_R (at $y = L_y$) [14]:

$$f(\vec{v}) = \frac{1}{\sqrt{2\pi}} \left(\frac{m}{k_B T_W} \right)^{3/2} |v_y| \exp\left(-\frac{m\vec{v}^2}{2k_B T_W} \right) \tag{1}$$

where T_W is the temperature (T_L or T_R) of the wall on which the collision occurs. During each collision, energy is exchanged between the system and the bath. In the steady state, the average heat current flowing through the system can, therefore, be found easily by computing the net heat loss from the system to the two baths (say Q_L and Q_R respectively) during a large time interval τ. The steady-state heat current is given by $\langle J \rangle = \lim_{\tau\to\infty} Q_L/\tau = -\lim_{\tau\to\infty} Q_R/\tau$. In the steady state the heat current (the heat flux density integrated over x) is independent of y. This is a requirement coming from current conservation. For a homogeneous system, $j_E = \langle J \rangle / L_x$. However, if the system has inhomogeneities then the flux density itself can have a spatial dependence, and in general we can have $j_E = j_E(x, y)$. In our simulations we have looked at $j_E(x, 0)$ and $j_E(x, L_y)$.

3. Results

The system is first allowed to reach the steady state in a temperature gradient with the two walls at right and left being maintained at temperatures of $k_B T_R = 1.5$ and $k_B T_L = 0.5$ such that the current density integrated over the whole x-range is the same at all y. The local temperature can be defined as $k_B T(y) = \langle 1/2\, m v^2(y) \rangle$, where the averaging is done locally over strips of width $d = 1$ and length L_x. If local thermal equilibrium (LTE) is maintained, we should have $\langle v^4(y) \rangle = 8(k_B T(y)/m)^2$. We find $k_B T(y)$ and $\langle v^4(y) \rangle$ as a function of distance y from the cold to the hot reservoir (figure 1(b)). From figure 1(b) it is evident that the temperature profile is almost linear in the single-phase regions, with a sharp increase near the interfaces, and LTE is approximately valid in all regions. With increased μ, the temperature difference between the edges of the solid region decreases, indicating an enhancement of the heat conductance within the solid. The temperature jumps at the interfaces are a measure of the Kapitza or contact resistance (R_K) [12], defined as

$$R_K = \frac{\Delta T}{j_E}, \tag{2}$$

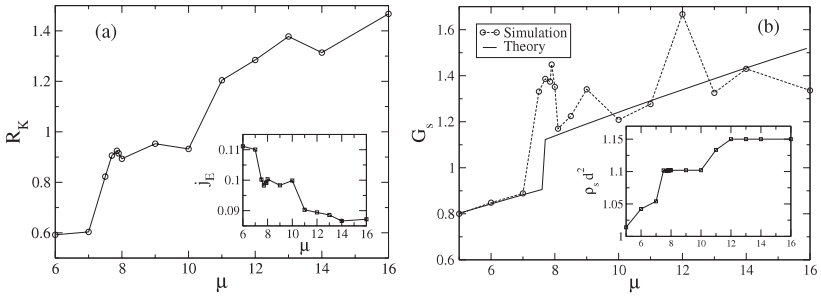

Figure 2. (a) The plot of the Kapitza resistance, R_K, expressed in units of $\tau_s d$, as a function of the potential depth μ, shows a jump at the layering transition. (b) Plot of the thermal conductance of the solid region, G_s (in units of $(\tau_s d)^{-1}$) as a function of μ. The points denote simulation data and the solid line a free-volume-type calculation of heat conductance $[G_s]_{fv}$. The inset shows the corresponding change in the solid density $\rho_s d^2$.

where ΔT is the difference in temperature across the interface. The Kapitza resistance increases with increasing trapping potential. It is evident that the interfaces are the regions of the highest resistance in the system. This large resistance can be traced back to large density mismatch at the contact of two phases. In figure 1(c) we plot the local density profile $\rho(y)d^2$. The trapping region shows large density corresponding to the solid. Also the colder liquid near the reservoir on the left shows a larger density than the hotter liquid near the one on the right. In figure 1(d) we plot the local compressibility $\kappa_T(y)$ defined via $\kappa_T = \rho^{-2}(\partial\rho/\partial\mu)_T$. Surprisingly, the compressibility of the interfaces is very large, making the narrow solid region also unusually compressible, pointing to the presence of large local number fluctuation.

In figure 2(a) we have plotted the Kapitza resistance R_K across the solid–liquid interface, averaged over the two interfaces, as a function of the strength of the external potential μ. The inset of figure 2(a) shows the heat flux through the system as a function of μ. As μ increases, the atoms from the surrounding liquid get attracted into the potential well and the density of the liquid becomes lower. The density mismatch at the solid–liquid interface therefore increases progressively. This figure shows a fairly sharp increase in R_K as well as a sharp decrease in current density j_E near $\mu = 8$ and 12. As we will see later, these are the μ-values at which the solid undergoes two types of layering transitions.

In figure 2(b) we show the heat conductance in the solid region G_s as a function of strength of the trapping potential μ. The inset in figure 2(b) shows the change in the averaged density of the solid region $\rho_s d^2$. The thick solid line in figure 2(b) is an analytical estimate obtained from a free-volume-type calculation [17] to be discussed in the next section. The $\rho_s d^2$–μ plot shows clear staircase-like sharp increases near the same values of μ ($\approx$8 and 12) where sharp changes in thermal conductance occur. With increase in the strength of the trapping potential, we observe two modes of density enhancement. (A) A whole layer of particles enters to increase the number of lattice planes in the y-direction. This happens, for example, as μ is increased from 7 to 8. Thus in this mode the separation of lattice planes parallel to the liquid–solid interface decreases (see figure 3(a)). (B) Each of the lattice planes parallel to the interface grows by an atom, thereby decreasing the interatomic separation within each lattice plane. This happens, for example, as one increases μ from 10 to 12 (see figure 3(c)). These two modes of density fluctuations leave their signatures by enhancing the heat conductance G_s, the effect of (A) being more pronounced than that of (B).

With increase in μ, these two modes alternate one after another, allowing the system to release extra stress developed due to particle inclusion in one direction in one cycle, by

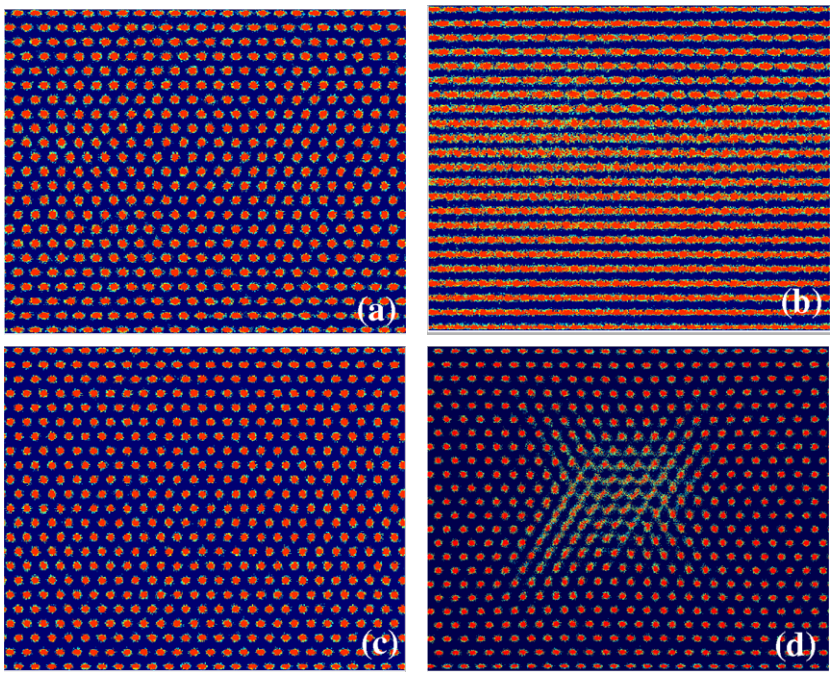

Figure 3. Overlapped density plot of 500 configurations in the region trapped by external potential μ. (a) A 23 × 23 triangular lattice solid formed from a 23 × 22 triangular lattice as the potential is increased from $\mu = 7$ to 8. (b) Local density peaks hop in the x-direction to incorporate >23 particles in lattice planes in response to the increased potential $\mu = 11$. (c) A 24 × 23 triangular lattice solid at $\mu = 12$. Notice the increase in particle numbers in the lattice planes. (d) Configuration obtained after $1.5 \times 10^4 \delta t$ as a 24 × 23 steady-state solid at $\mu = 16$ is quenched to $\mu = 24$. This shows a dislocation pair—a 23-layered region trapped in between a 24-layered solid. At steady state (after a time $10^5 \delta t$), dislocations annihilate to produce a 24 × 24 triangular lattice solid. Colour code: blue (dark): low density; red (light): high density.

inclusion of particles in the perpendicular direction in the next cycle. Finally, at large enough μ the density of the solid region saturates, ending the cycles. It is also interesting to observe how the particles accommodate themselves going from figures 3(a)–(d). We find strained triangular solids with 23×23, 24×23 and 24×24 unit cells at $\mu = 8$, 12 and 24 respectively (see figure 3). In the intermediate configurations one observes metastable dislocation pairs (figure 3(d)) and peaks in the local particle density which correspond to a few particles rapidly oscillating between two neighbouring positions (figure 3(b)) in order to maintain commensurability. Such rapid, localized, particle fluctuations may be observable in experiments.

The layering transition in the solid by process (A) occurs via metastable dislocation formation and annihilation by incorporating particles from the liquid region. The kinematics of dislocation generation, transport and decay is controlled by diffusion, which is a very slow process [7] in a solid compared to particle collision and kinetic energy transfer times. Thus it is possible for a system with metastable dislocation pairs to reach an effective thermal steady state. Figure 3(d) shows overlapped configurations of the solid region containing a dislocation–antidislocation pair, as the system is quenched from $\mu = 16$ to 24. The overlapped configurations are separated by time $100\delta t$ and collected after a time of $1.5 \times 10^4 \delta t$ after the quench. At this stage the system is in a metastable state though, at the same time, maintaining LTE, which we check by computing $\langle v^4(y) \rangle$ and $k_B T(y)$ locally. This gives a heat conductance

$G_s = 2.29\ (\tau_s d)^{-1}$. After a further wait for $10^5 \delta t$, the dislocations get annihilated. At this stage the whole solid region is transformed into an equilibrium 24×24-triangular lattice. On measuring the heat conductance now, we obtain $G_s = 3.53\ (\tau_s d)^{-1}$. Thus with the annihilation of a single dislocation pair the conductance of the solid rises by about 54%! Metastable configurations with dislocation pairs, therefore, have strikingly different thermal properties in this small system. Note that in the present system, configurations containing dislocations are always metastable since dislocations are either annihilated or are lost at the interface [2].

4. Free-volume theory

Finally, we provide a brief sketch of an approximate theoretical approach for calculating heat conductance within the solid region. A detailed treatment of this approach is available in [17]. The continuity of the energy density can be utilized to obtain an exact expression for the αth component of the heat flux density,

$$\begin{aligned} j_\alpha(\mathbf{r}) &= j_\alpha^K(\mathbf{r}) + j_\alpha^U(\mathbf{r}) \\ &= \sum_i \delta(\mathbf{r} - \mathbf{r}_i) h_i \mathbf{v}_i^\alpha + \tfrac{1}{2} \sum_{i, j \neq i} \theta(x_i^\alpha - x^\alpha) \prod_{\nu \neq \alpha} \delta(x^\nu - x_i^\nu) f_{ij}^\beta (v_i^\beta + v_j^\beta). \end{aligned} \tag{3}$$

Here $\theta(x)$ is the Heaviside step function, $\delta(\cdots)$ is a Dirac delta function, $h_i = m\mathbf{v}_i^2/2 + \phi(\mathbf{r}_i) + \sum_{i>j} u(r_{ij})$, $\phi(\mathbf{r}_i)$ is an onsite potential and $u(r_{ij})$ is interparticle interaction. The first term in equation (3), $j_\alpha^K(\mathbf{r})$, denotes the amount of energy carried by particle flux (convection), and $j_\alpha^U(\mathbf{r})$ denotes the net rate at which work is done by particles on the left of x^α on the particles on the right (conduction). The αth component of the integrated heat current density over the solid region is

$$\langle I_\alpha \rangle = \sum_i \langle\, h_i v_i^\alpha \rangle - \frac{1}{4} \sum_{i, j \neq i} \left\langle \frac{\partial u(r_{ij})}{\partial r_{ij}} \frac{x_{ij}^\alpha x_{ij}^\beta}{r_{ij}} (v_i^\beta + v_j^\beta) \right\rangle. \tag{4}$$

In this study we focus on the average heat current density along the y-direction, $j_E = \langle I_y \rangle / L_x L_s$. We assume LTE and ignore conductance inside the solid [17]. Then assuming the conductance of our present system to be simply proportional to that of a hard disc system with an effective diameter σ, the heat conductance in units of $(\tau_s d)^{-1}$ can be expressed as

$$G_s = \frac{j_E}{\Delta T} = \left[3 \frac{\rho_s}{L_s} \frac{y_c^2}{\tau_c} \right] \left(\frac{d}{\sigma} \right)^2 \tag{5}$$

where ρ_s is the average density of the solid, y_c is the average separation between the colliding particles in the y-direction and τ_c is the mean collision time. The extra factor of $(d/\sigma)^2$ is due to the mapping of the soft discs of diameter d to effective hard discs of diameter σ.

We estimate y_c^2 and τ_c from the fixed-neighbour free-volume theory as in [17]. Briefly, we assume that a (hard) test particle moves in the fixed cage formed by the average positions of its neighbours and obtain the average values $[y_c^2]_{fv}$ from geometry and the timescale $[\tau_c]_{fv} = c\sqrt{V_{fv}/k_B T}$, where V_{fv} is the available free volume of the test particle moving with a velocity derived from the temperature $k_B T$. The effective hard disc diameter σ and the constant c of $\mathcal{O}(1)$ are both treated as fitting parameters. Using $k_B T = 1$, $d/\sigma = 1.13$ and $c = 0.4$ we obtain a fit to the G_s–μ curve with a layering transition from 22 to 23 layers near $\mu = 8$. The fitted result, depicted as the solid line in figure 2(b), is seen to reproduce most of the qualitative features of the simulation results, especially the jump in conductance due to the layering transition.

5. Conclusions

We have shown that details of the structure have a measurable effect on the thermal properties of the trapped solid lying in contact with its liquid. In this study, we were particularly interested in exploring the impact of structural changes, namely the layering transitions, on heat transport. One must, however, remember that the layering transition is a finite size effect [2], and it gets progressively less sharp as one goes to very large channel widths. An important consequence of this study is the possibility that the thermal resistance of interfaces may be altered using an external potential which causes layering transitions in a trapped nanosolid. We have shown that metastable dislocations drastically reduce the conductance of an otherwise defect-free nanosized solid. Recently, electrical [18] and thermal [17] transport studies on confined solid strips have also revealed strong signatures of such structural transitions due to imposed external strain. We believe that these phenomena have the potential for useful applications, for example as tunable thermal switches or in other nano-engineered devices.

We would like to thank Madan Rao, Abhishek Dhar, Tamoghna K Das, Kurt Binder, Andrea Ricci and Peter Nielaba for discussions and Martin Zapotocky for a critical reading of the manuscript. This work was partially supported by the Department of Science and Technology and CSIR (India).

References

[1] Cahill D G *et al* 2003 *J. Appl. Phys.* **93** 793
[2] Chaudhuri A, Sengupta S and Rao M 2005 *Phys. Rev. Lett.* **95** 266103
[3] Metcalf H J and van der Straten P 1999 *Laser Cooling and Trapping* (Heidelberg: Springer)
[4] Phillips W D 1998 *Rev. Mod. Phys.* **70** 721
[5] Grier D G 2003 *Nature* **424** 810
[6] Haghgooie R and Doyle P S 2004 *Phys. Rev.* B **70** 061408
[7] Chaudhuri D and Sengupta S 2004 *Phys. Rev. Lett.* **93** 115702
[8] Ricci A, Nielaba P, Sengupta S and Binder K 2006 *Phys. Rev.* E **74** 010404
[9] de Gennes P G 1990 *Langmuir* **6** 1448
[10] Barrat J-L and Chiaruttini F 2003 *Mol. Phys.* **101** 1605
[11] Kapitza P L 1941 *J. Phys. USSR* **4** 181
[12] Pollack G L 1969 *Rev. Mod. Phys.* **41** 48
[13] Lippi A and Livi R 2000 *J. Stat. Phys.* **100** 1147
[14] Bonetto F, Lebowitz J and Rey-Bellet L 2000 *Mathematical Physics 2000* ed A Fokas *et al* (London: Imperial College Press) p 128
[15] Grassberger P and Yang L 2002 *Preprint* cond-mat/0204247
[16] Frenkel D and Smit B 2002 *Understanding Molecular Simulation* 2nd edn (New York: Academic)
[17] Chaudhuri D and Dhar A 2006 *Phys. Rev.* E **74** 016114
[18] Datta S, Chaudhuri D, Saha-Dasgupta T and Sengupta S 2006 *Europhys. Lett.* **73** 765